



## Co-mixing Hydrogen and Methane May Double the Energy Storage Capacity

Journal:	<i>Journal of Materials Chemistry A</i>
Manuscript ID	TA-ART-02-2018-001909.R1
Article Type:	Paper
Date Submitted by the Author:	18-Mar-2018
Complete List of Authors:	Xue, Qianqian; Huazhong University of Science and Technology Wu, Menghao; Huazhong University of Science and Technology, School of Physics and Wuhan National High Magnetic Field Center Zeng, Xiao; University of Nebraska-Lincoln, Chemistry Jena, Purusottam; Virginia Commonwealth University, Physics Department

## Co-mixing Hydrogen and Methane May Double the Energy Storage Capacity

Qianqian Xue<sup>a</sup>, Menghao Wu<sup>a\*</sup>, Xiao Cheng Zeng<sup>b\*</sup>, Puru Jena<sup>c</sup>

<sup>a</sup>School of Physics and Wuhan National High Magnetic Field Center, Huazhong University of Science and Technology, Wuhan 430074, China

<sup>b</sup>Department of Chemistry, University of Nebraska-Lincoln, Lincoln, NE 68588, USA

<sup>c</sup>Department of Physics, Virginia Commonwealth University, Richmond, VA 23284, USA

**Abstract** The use of hydrogen fuel as clean energy is hindered by the low capacity of the storage medium. Although the combustion energy of a CH<sub>4</sub> molecule is three times higher than that of H<sub>2</sub>, the same medium can adsorb much fewer CH<sub>4</sub> molecules than H<sub>2</sub> due to the much stronger inter-molecular repulsion of the former. Here, we show, from first-principles theoretical calculations, that mixing hydrogen and methane gas may significantly increase the energy storage capacity compared with either pure hydrogen or methane. The repulsion between hydrogen and methane molecules is moderate and the open metal sites on a surface can be effectively used to increase the energy storage capacity. Using two different surfaces (graphene and graphene nano ribbons) decorated with alkali and 3d transition metal atoms, as examples, we show that the energy storage capacity can be approximately doubled by this mixing and an equivalent hydrogen gravimetric density of 14.0 wt% can be obtained. This approach can be applied to most current storage media with open metal sites.

## 1. Introduction

In 2017, the U.S. Department of Energy (DOE) launched Hydrogen at Scale (H2@Scale) to explore the potential for large scale hydrogen production, utilization, and storage. Also launched is Advance Research Consortium (HyMARC) to address the key barriers impeding the development of a hydrogen economy<sup>1</sup>. Hydrogen, as a clean energy solution to mitigate the environmental concern over fossil fuels, has been explored for decades because of its natural abundance, high energy density, and non-polluting nature; water is the only chemical by-product. However, for the hydrogen economy to succeed, one must identify safe and cost-effective hydrogen storage materials, required for hydrogen fuel-cell powered systems. A target of 5.5 wt% has been set by the U.S. DOE for the storage medium. Although many systems meet this requirement, no practical storage medium has emerged that is reversible and where hydrogen sorption can take place at ambient conditions.<sup>2,3</sup> The ideal adsorption energy of H<sub>2</sub> should lie within 0.2-0.6 eV per molecule.<sup>4,5</sup> Theoretically, a number of material designs have been proposed that meet this goal.<sup>6-8</sup> A class of these materials is transition-metal-decorated nanostructures<sup>9-12</sup> where hydrogen is bound in quasi-molecular form through the Kubas interaction. The binding energies in these cases lie in the range of 0.5 to 0.8 eV/H<sub>2</sub> molecule.<sup>13</sup> For surfaces decorated with alkali metal atoms, H<sub>2</sub> also binds in quasi-molecular form, but through a charge polarization mechanism.<sup>14,15</sup> Here, the adsorption energies lie in the range of 0.1-0.3 eV/H<sub>2</sub> molecule.<sup>16-22</sup> Even for those theoretical predictions for ideal conditions, a hydrogen storage gravimetric capacity higher than 10 wt% has been scarcely obtained.<sup>19</sup>

An alternative to hydrogen may be methane storage. Note that the combustion heat for hydrogen, namely 141.8 MJ/kg is much higher than that of methane, namely, 55.5 MJ/kg, and

also hydrogen-natural gas (HCNG) mixtures have been used as fuels in internal combustion engines.<sup>23</sup> However, because the mass of each methane molecule is about eight times larger than that of a hydrogen molecule, the combustion of one methane molecule would produce about 3.1 times the heat produced by a hydrogen molecule. Consequently, methane adsorption on similar open metal sites has been explored both theoretically and experimentally, with particular emphasis on metallo-organic frameworks (MOFs).<sup>24-32</sup> Generally, compared with hydrogen storage, the same medium may store methane with less volumetric capacity, but with more gravimetric capacity. For example, the methane storage capacity of MOFs summarized in a previous review<sup>25</sup> is less than 20 wt%. Note that the much stronger repulsion between methane molecules compared with hydrogen molecules, prevents multiple methane molecules from gathering at one open metal site. Typically, each open metal site of the storage medium may adsorb 2-4 hydrogen molecules, but only 1~2 methane molecules.

In this paper we propose that co-mixing hydrogen and methane gas may give rise to a much higher energy capacity compared with storage of either pure hydrogen or pure methane. Our first-principles calculations reveal that the repulsion between hydrogen and methane molecule is moderate for high-density storage. Thus, the open metal sites on a surface can be efficiently utilized by this mixing and the energy capacity can be greatly enhanced. Charge analysis also reveals that both the stronger Coulomb interaction and induced multipole moment may contribute to the increase in capacity. Two examples are selected as benchmark from previous DFT studies where their stability against metal clustering had already been verified: (1) For graphene decorated with alkali ions that can each adsorb 2~3 H<sub>2</sub> molecules, the energy density can be doubled by substituting one 1 H<sub>2</sub> molecule by one CH<sub>4</sub> molecule at each metal site. (2) For

graphene nano ribbon decorated with 3d transition metal where 4-5 H<sub>2</sub> can be adsorbed on each metal site, substitution of two H<sub>2</sub> molecules by two CH<sub>4</sub> molecules at each open metal site may render an equivalent hydrogen gravimetric density as high as 14.0wt%.

## 2. Methods

Calculations based on density-functional-theory (DFT) were performed using the Vienna *ab initio* Simulation Package (VASP)<sup>33,34</sup> and the projector augmented wave (PAW) method.<sup>35</sup> The exchange–correlation potential was treated using the Perdew–Burke–Ernzerhof (PBE) functional<sup>36</sup> within the generalized gradient approximation (GGA). The van der Waals dispersive force was accounted for using the PBE-D2 functional of Grimme.<sup>37</sup> The electron wave functions were expanded in terms of plane waves with a kinetic energy cutoff of 400 eV to attain the required convergence. The forces on all atoms were converged to at least 0.005 eV/Å. For calculations of the interaction between two gas molecules, a rectangle unitcell of 16×16×20 Å was adopted where the interaction from adjacent image supercell will be negligible. For Li-decorated graphene, a uniform (2 × 2) graphene supercell was used with an in-plane lattice parameter of 4.920 Å and the K-points mesh of 8 × 8 × 1 based on Monkhorst - Pack scheme. For Sc-decorated graphene nanoribbon, the K-points mesh is 1 × 1 × 7. A vacuum region of 20 Å was applied in the direction perpendicular to the graphene plane to avoid interactions between two neighboring images.<sup>38</sup> The average binding energies of H<sub>2</sub> and CH<sub>4</sub> in the co-mixed samples with *n* H<sub>2</sub> and *m* CH<sub>4</sub> molecules are, respectively, defined as,

$$\bar{E}_{an} = [E(\text{medium} + m \text{CH}_4) + n E(\text{H}_2) - E(\text{medium} + n \text{H}_2 + m\text{CH}_4)]/n$$

$$\bar{E}_{bm} = [E(\text{medium} + n \text{H}_2) + m E(\text{CH}_4) - E(\text{medium} + n \text{H}_2 + m\text{CH}_4)]/m$$

Here,  $E(\text{medium} + n \text{H}_2) / E(\text{medium} + m \text{CH}_4)$  is the total energy of the medium with *n*

adsorbed  $H_2$  molecules/  $m$  adsorbed  $CH_4$  molecules;  $E(H_2) / E(CH_4)$  is the energy of isolated  $H_2/CH_4$ ;  $E(\text{medium} + n H_2 + mCH_4)$  is the total energy of the medium with  $n$  adsorbed  $H_2$  molecules and  $m$  adsorbed  $CH_4$  molecules. The positive binding energy corresponds to stable configuration and represents an exothermic adsorption process.

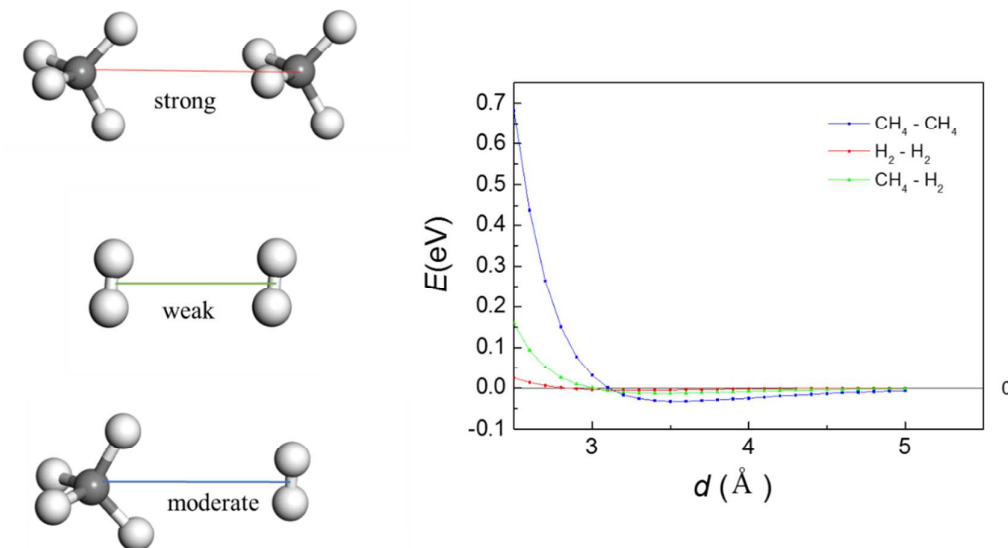


Figure 1 Computed PBE-D2 interaction energy between  $H_2 - H_2$ ,  $CH_4 - CH_4$ , and  $H_2 - CH_4$  as a function of inter-molecular distance. Grey and white spheres denote C and H atoms respectively.

### 3. Results and Discussions

#### 3.1 Interaction between $H_2$ and $CH_4$

To gain insight into the merit of co-mixing of hydrogen and methane, we begin with a discussion of the interaction between these molecules. In Fig. 1, we show the energies as a function of inter-molecular distance between  $H_2 - H_2$ ,  $CH_4 - CH_4$ , and  $H_2 - CH_4$ . Note that the interaction between methane molecules is much more repulsive than that between the hydrogen molecules for distances up to 3 Å. In addition, the optimized inter-molecular distances between

$\text{CH}_4$  molecules and  $\text{H}_2$  molecules are respectively 3.5 Å and 3.2 Å. This can be understood by analyzing the charges on the H atoms in Fig. S1. In  $\text{CH}_4$  dimer, the charges on the hydrogen atoms are positive, which results in a repulsive interaction, making the intermolecular distance large. The charges on the H atoms in the  $\text{H}_2$  dimer, on the other hand, are vanishingly small, making the bonding between these molecules weak, governed by polarization forces. The situation, however, is different when  $\text{H}_2$  interacts with  $\text{CH}_4$ . Here, the charges on the H atoms in  $\text{H}_2$  are negative while those in  $\text{CH}_4$  are positive, making them attract. Consequently, the intermolecular distance between  $\text{H}_2$  and  $\text{CH}_4$  is shorter (namely, 3.4 Å) than that between  $\text{CH}_4$  molecules. In addition, the binding energy of  $\text{H}_2$ - $\text{CH}_4$  (~14 meV) is larger than that between two  $\text{H}_2$  molecules (~6 meV). The large size of  $\text{CH}_4$  will make it difficult to decorate many  $\text{CH}_4$  molecules around an open metal site due to steric hindrance, even though the binding energy between two  $\text{CH}_4$  molecules is larger than that between  $\text{H}_2$  and  $\text{CH}_4$ .

There is also another reason why co-mixing of  $\text{H}_2$  and  $\text{CH}_4$  may lead to an increase in energy density. The adsorption energy of a hydrogen or methane molecule at an open metal site usually ranges between 0.1 and 0.4 eV, and the optimized metal-molecule distance is usually around 2.0-2.5 Å. When multiple gas molecules are adsorbed, the repulsion energy between gas molecules should be less than ~0.1 eV so that the overall average adsorption energy can still be above 0.2 eV. However, the repulsion energy between the methane molecules increases drastically above 0.1 eV when  $\text{CH}_4$  -  $\text{CH}_4$  distance is reduced below 2.85 Å, which would approximately be the minimum distance between methane molecules adsorbed at the same open metal site. In comparison, the repulsion energy between a  $\text{H}_2$  and a  $\text{CH}_4$  at the same distance is only ~0.02 eV, and the  $\text{H}_2$  -  $\text{CH}_4$  distance can be reduced to 2.55 Å, with repulsion

energy below  $\sim 0.1$  eV.

### 3.2 Interaction of H<sub>2</sub> and CH<sub>4</sub> with a substrate

For practical storage, it is necessary to first understand how the gas molecules interact with a substrate. Taking graphene as an example we have calculated the adsorption energies of H<sub>2</sub> and CH<sub>4</sub> as a function of distance from the substrate. The results are plotted in Fig. 2. Note that the interaction between CH<sub>4</sub> and graphene is much more repulsive than that between H<sub>2</sub> and graphene, although CH<sub>4</sub> is bound more strongly to the graphene substrate than H<sub>2</sub>. The adsorption energy of the former CH<sub>4</sub> is  $\sim 0.12$  eV, while that of H<sub>2</sub> is  $\sim 0.06$  eV. Similarly, the distance between CH<sub>4</sub> and the substrate, namely, 3.4 Å is also much larger than that between H<sub>2</sub> and the substrate, which is 2.8 Å.

### 3.3 Interaction of H<sub>2</sub> and CH<sub>4</sub> with a Li atom supported on graphene

It has been demonstrated earlier that metal atoms supported on a substrate can bind multiple H<sub>2</sub> molecules. To study how co-mixing of H<sub>2</sub> and CH<sub>4</sub> will affect this binding, we have investigated the trapping of H<sub>2</sub>, CH<sub>4</sub>, and their mixtures at Li sites supported on a graphene substrate. There are two factors to consider. Due to charge transfer between Li and the graphene substrate, the Li sites may become ionic, which in turn can bind the gas molecules through the polarization mechanism. This factor as well as the interaction of the gas molecules with the substrate may affect not only the strength of their binding but also the number of gas molecules that can be trapped at each metal site. A schematic model for the adsorption of two molecules around a Li metal site is illustrated in Fig. 2(b) and (c). The characteristic distances to consider are the inter-molecular distance,  $l$ ; the distance between the molecule and the metal atom,  $s$ ; and the distance between the metal atom and the substrate,  $h$ . It is known that the intermolecular

distance between  $\text{CH}_4$  molecules,  $l > \sim 2.9 \text{ \AA}$  and the distance between  $\text{CH}_4$  and an open metal site,  $s < \sim 2.5 \text{ \AA}$ . If a metal site is supported on a substrate like graphene at a distance of  $\sim 2.0 \text{ \AA}$ , the repulsive energy will overwhelm the adsorption energy, making adsorption difficult. To ensure both the adsorbed methane molecules are more than  $\sim 3.0 \text{ \AA}$  away from the substrate while less than  $\sim 2.5 \text{ \AA}$  away from the metal site, the metal ion should be at least  $\sim 1.0 \text{ \AA}$  away from substrate. Even these preconditions are met, the adsorption energy could still be below  $0.2 \text{ eV}$ , considering all the repulsion from other methane molecules either at the same metal site or adjacent metal sites (which can be considerable in the case of high density of open metal sites), and also from the substrate. In comparison,  $\text{H}_2$  can approach the substrate at much shorter distance with repulsion energy from substrate less than  $0.1 \text{ eV}$ . The repulsion from adjacent hydrogen or methane molecules are also much weaker. The optimized ground state of the adsorbed  $\text{CH}_4$ - $\text{H}_2$  pair is likely to be the configuration in Fig. 2(c), where  $\text{H}_2$  is much closer to the substrate than  $\text{CH}_4$  and the  $\text{CH}_4$ - $\text{H}_2$  distance could be large to minimize repulsion.

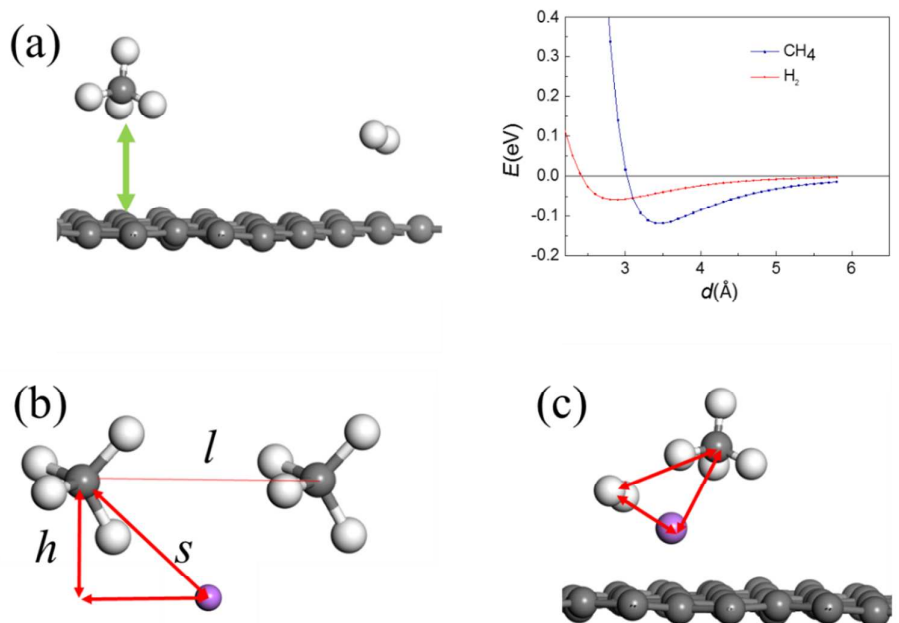


Figure 2 (a) Adsorption energy as a function of distance between CH<sub>4</sub>/H<sub>2</sub> and graphene. (b) and (c) are respectively schematic illustrations of CH<sub>4</sub>- CH<sub>4</sub> and CH<sub>4</sub>- H<sub>2</sub> pair adsorbed at an open metal site denoted by a purple sphere.

This schematic model should apply to various alkali-metal-doped carbon-based materials such as fullerene,<sup>16, 39</sup> carbon nanotube,<sup>18</sup> or graphene<sup>17, 40</sup> decorated with lithium ions. Here following Ref. 39, we choose graphene as a prototype medium for hydrogen/methane storage. As shown in Fig. 3(a), graphene is decorated by Li ions on both sides for a maximum adsorption capacity of hydrogen molecules. The charge and binding energy of each Li ion are respectively +0.19e and 1.63 eV. According to Table 1, the average adsorption energy when each Li ion adsorbs 1, 2, and 3 H<sub>2</sub> are, respectively, 0.07, 0.24 and 0.21 eV per H<sub>2</sub>, which indicates that the adsorption energy of the 1<sup>st</sup>, 2<sup>nd</sup>, and 3<sup>rd</sup> H<sub>2</sub> will be respectively 0.07eV,  $0.24 \times 2 - 0.07 = 0.41$  eV,  $0.21 \times 3 - 0.24 \times 2 = 0.15$  eV. As a result, the number of effectively adsorbed H<sub>2</sub> will be 2 for each Li

atom, and the overall weight capacity of hydrogen storage will be 6.8 wt%.

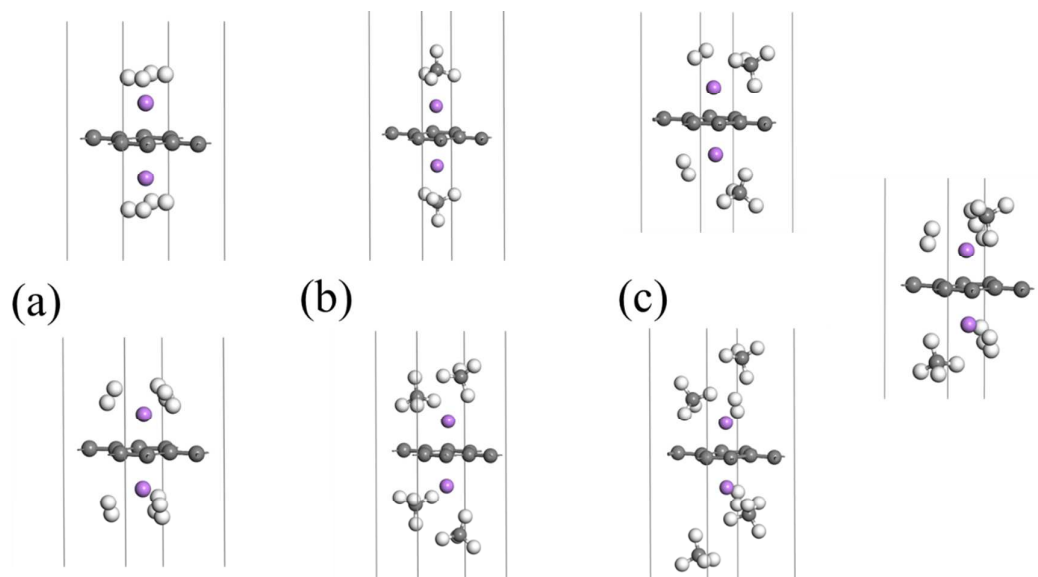


Figure 3 Graphene decorated with Li ions with adsorption of (a) 1 and 2 H<sub>2</sub>; (b) 1 and 2 CH<sub>4</sub>; (c) 1

H<sub>2</sub>+ 1 CH<sub>4</sub>, 1 H<sub>2</sub>+ 2 CH<sub>4</sub>, and 2 H<sub>2</sub>+ 1 CH<sub>4</sub> per Li ion.

Table 1. Average binding energy of H<sub>2</sub> / CH<sub>4</sub> for mixing adsorption of  $n$  H<sub>2</sub> molecule and  $m$  CH<sub>4</sub>.

<b><math>n</math></b>	1	2	3		1	2	1	
<b><math>m</math></b>				1	2	1	1	2
<b><math>E_{an}</math>(eV)</b>	0.07	0.24	0.18			0.20	0.22	0.17
<b><math>E_{bm}</math>(eV)</b>				0.28	0.21	0.41	0.22	0.26

For methane storage, as shown in Fig. 3(b), the adsorption energy for the 1<sup>st</sup> and 2<sup>nd</sup> CH<sub>4</sub> molecule at a Li site will be 0.28 and 0.14 eV, where the 2<sup>nd</sup> CH<sub>4</sub> is not likely to be adsorbed at ambient conditions. The distance between two methane molecules is 3.25 Å, slightly larger than the CH<sub>4</sub> – CH<sub>4</sub> distance limit of 2.85 Å estimated above. The distances of these molecules from

graphene are, respectively, 3.0 and 4.4 Å. While the 1<sup>st</sup> CH<sub>4</sub> is right at the limiting distance of 3.0 Å, estimated above; their distances from the Li ion are, respectively 2.3 and 2.8 Å. The large distance of 2.8 Å from Li indicates that the adsorption of the 2<sup>nd</sup> CH<sub>4</sub> is much weaker. If a (4 × 4) graphene supercell is adopted to study a low-density condition where the distance between adjacent Li ions at one side is doubled, the 2<sup>nd</sup> CH<sub>4</sub> at a Li site can be adsorbed due to much less repulsion from adjacent supercell, while the 3<sup>rd</sup> CH<sub>4</sub> will still be repelled away from the Li ion. Even here the maximum number of adsorbed CH<sub>4</sub> is doubled, the density of Li ions as well as the methane capacity will be much lowered.

Now we try to enhance the energy capacity by co-mixing hydrogen and methane. If every Li ion adsorbs one hydrogen and one methane molecule as in Fig. 3(c), the average adsorption energy will be 0.24 eV per molecule, according to Table 1. Moreover, when one more H<sub>2</sub> or CH<sub>4</sub> is added at each open metal site, every Li atom would bind two H<sub>2</sub> and one CH<sub>4</sub>. The average adsorption energy of 0.23 eV is within the desirable range for storage. Considering that combustion heat of one CH<sub>4</sub> is 3.1 times that of H<sub>2</sub>, the stored energy is equivalent to hydrogen gravimetric density of 13.6 wt%. This is twice the density compared with pure hydrogen storage. Here, the distances away from graphene are, respectively, 2.4/2.3 Å and 4.1 Å for H<sub>2</sub> and CH<sub>4</sub>, which is consistent with the model shown in Fig. 2(c). For one H<sub>2</sub> and two 2CH<sub>4</sub> adsorbed on every Li site, the average adsorption energy is 0.20 eV, which is in the required range for effective adsorption. However, here the 3<sup>rd</sup> CH<sub>4</sub> is already repelled to 4.1 Å away from the Li ion. With an adsorption energy of only 0.12 eV, it is unlikely that it will remain bound at ambient conditions.

Generally, for open metal sites, the unscreened Coulomb interaction plays an important role in the adsorption of hydrogen molecules, while the adsorption of methane is mainly attributed to

the charge redistribution and induced multipole moments.<sup>28</sup> We performed Hirshfeld charge analysis on the structures of Fig. 3(b) and (c) to compare the storage of pure methane vs co-mixed H<sub>2</sub> and CH<sub>4</sub>. The charge on every atom is listed in Fig. S1 of supporting information: the total charge on each methane molecule is  $\sim -0.01e$  upon the adsorption of one CH<sub>4</sub> per Li ion in Fig. 3(b). This charge becomes  $\sim 0.03e$  in Fig. 3(c) when one more H<sub>2</sub> is added. Upon the adsorption of two CH<sub>4</sub> molecules per Li ion, the total charge on the methane molecule closer to Li is  $\sim -0.01e$ , while it is  $-0.03e$  for the one farther to Li in Fig. 3(b). Similar results are found for the system in Fig. 3(c). The charge on methane molecule close to Li ion will turn from negative to positive upon the co-adsorption of hydrogen molecule. This is revealed from the following calculations. When one H<sub>2</sub> and one CH<sub>4</sub> are placed in the same supercell, there will be a charge of  $\sim 0.01e$  transferred from H<sub>2</sub> to CH<sub>4</sub>. However, the symmetry of a CH<sub>4</sub> is also reduced as revealed by the charge distribution on its four H atoms. For one CH<sub>4</sub> adsorbed per Li ion in Fig. 3(b), the charge on H atoms of CH<sub>4</sub> range from 0.026e to 0.034e; for one CH<sub>4</sub> and one H<sub>2</sub> per Li ion in Fig. 3(c), the charge on H atoms of CH<sub>4</sub> range from 0.026e to 0.043e, so the dipole moment is enhanced upon mixing storage. As a result, both Coulomb interaction and induced multipole moment may contribute to the adsorption energy of co-mixed methane and hydrogen.

### **3.4 Interaction of H<sub>2</sub> and CH<sub>4</sub> around a Sc atom supported on armchair graphene nano ribbon (AGNR)**

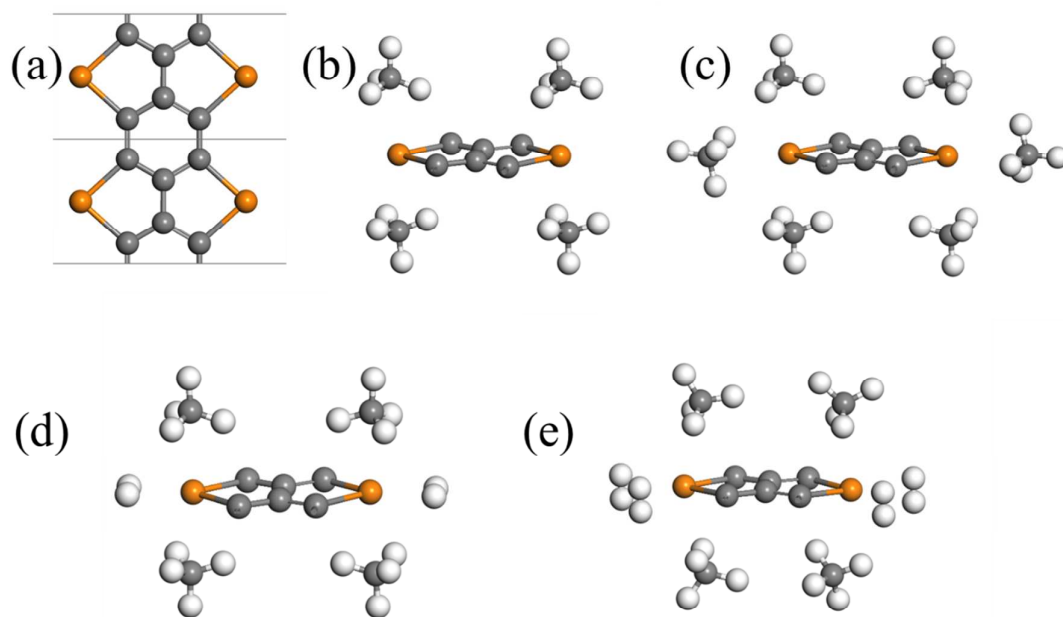


Figure 4 (a) AGNR with edges decorated with Sc atoms (denoted by orange spheres) and adsorption of (b) 2 CH<sub>4</sub>; (c) 3 CH<sub>4</sub>; (d) 1 H<sub>2</sub>+ 2 CH<sub>4</sub>, and (e) 2 H<sub>2</sub>+ 2 CH<sub>4</sub> per Sc ion.

Table 2. Average binding energy of H<sub>2</sub> / CH<sub>4</sub> for mixing adsorption of n H<sub>2</sub> molecule and m CH<sub>4</sub>.

<b>a</b>	4			1	2
<b>b</b>		2	3	2	2
<b>E<sub>a</sub>(eV)</b>	0.27			0.26	0.26
<b>E<sub>b</sub>(eV)</b>		0.22	0.19	0.31	0.28

The above model can be applied to various medium decorated by alkali ions: each ion can generally adsorb 2~3 H<sub>2</sub> for hydrogen storage, and the energy density can be approximately doubled upon the substitution of 1 H<sub>2</sub> by 1 CH<sub>4</sub>. However, when 3d transition metal ions are used, the binding of the gas molecules is enhanced compared with alkali ions and each 3d metal atom can adsorb 4-5 H<sub>2</sub> molecules, provided there is enough room around the open metal site. In this case, more H<sub>2</sub> molecules may be substituted by CH<sub>4</sub> for higher capacity. Following the previous

DFT study<sup>10</sup> we consider armchair graphene nanoribbon (AGNR) with edges decorated by Sc., where the stability against metal clustering has already been verified in details. Since atomically precise bottom-up fabrication of ultra-narrow GNRs had been realized through polymerization of small molecules<sup>41</sup>, the narrowest GNR was chosen for study where the clean edges constructed from small molecules can give rise to strong binding energy of 3d metal adatoms<sup>42-45</sup>. In this case, the surface area around the metal open site at the edges is much larger compared with that in Li-decorated graphene, as shown in Fig. 4(a). In previous DFT study it was shown that each Sc ion can adsorb up to 4 H<sub>2</sub>, with hydrogen gravimetric density reaching 9.1 wt%.<sup>10</sup> For methane storage, the surface of each open metal site is already large enough for the adsorption of at least 2 CH<sub>4</sub>, distributed at both sides of the graphene plane, as shown in Fig. 4(b). The average adsorption energy of 0.22eV is within the desirable range. The adsorption energy for adding the 3<sup>rd</sup> CH<sub>4</sub>, however, is only 0.16 eV, which is slightly below the desired energy for adsorption. If CH<sub>4</sub> is substituted by 1 or even 2 H<sub>2</sub>, the adsorption energies for the 1<sup>st</sup> and 2<sup>nd</sup> H<sub>2</sub> are, respectively, 0.31 and 0.21eV. As a result, considering that combustion heat one CH<sub>4</sub> is 3.1 times that of H<sub>2</sub>, the stored energy will be equivalent to hydrogen gravimetric density of 14.0 wt%.

#### 4. Conclusions

In summary, we show from first-principles calculations that mixing hydrogen and methane gas may give rise to a much higher energy capacity compared with pure hydrogen or methane storage. The repulsion between hydrogen and methane molecule at short distances is much less than that between methane molecules, and the open metal site on a surface can be effectively utilized to bind H<sub>2</sub> and CH<sub>4</sub>. As a result, the energy density can be greatly enhanced. Charge analysis reveals that both Coulomb interaction and induced multipole moment may contribute to

the stronger adsorption of co-mixed methane and hydrogen. For surfaces decorated by alkali ions like Li-decorated graphene, each metal site can each adsorb 2~3 H<sub>2</sub> molecules, and the energy density can be approximately doubled upon the substitution of one H<sub>2</sub> by one CH<sub>4</sub> at each metal site; for surfaces decorated with 3d transition metal atoms like AGNR decorated with Sc at its edges, 4-5 H<sub>2</sub> molecules can be adsorbed on each open metal site, and with two H<sub>2</sub> molecules substituted by two CH<sub>4</sub> at each open metal site, the hydrogen gravimetric density can reach 14.0wt%. This approach can be applied to other storage media such as MOFs with open metal sites and similar results are expected. Thus, co-mixing H<sub>2</sub> and CH<sub>4</sub> may offer an excellent opportunity to enhance the energy capacity, making a successful hydrogen economy within reach.

#### Supplementary Information

Supplementary Information is available from the RSC Online Library or from the author.

#### Acknowledgements

The work was supported by the National Natural Science Foundation of China (Nos. 21573084).

We thank Prof. Ju Li (MIT) for helpful discussions, We also thank Shanghai Supercomputing Center for providing computational resources. PJ acknowledges support by the U.S. Department of Energy, Office of Basic Energy Sciences, Division of Materials Sciences and Engineering under Award No. DE-FG02-96ER45579.

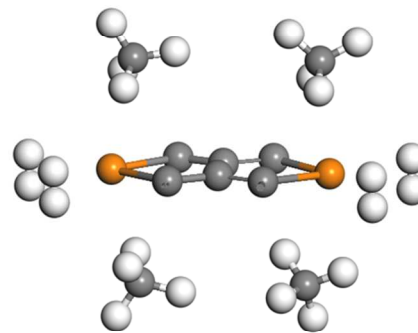
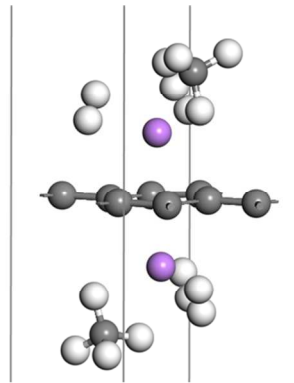
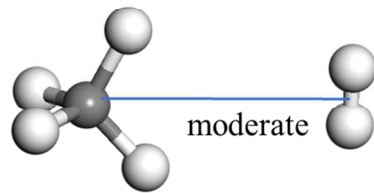
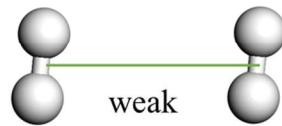
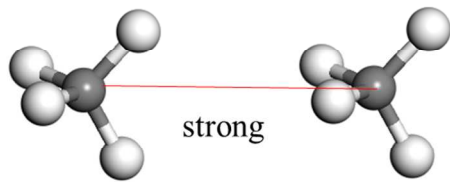
#### Notes and references

1. K. Morishige and T. Komura, *Langmuir*, 1998, **14**, 4887-4890.
2. P. Jena, *J. Phys. Chem. Lett.*, 2011, **2**, 206-211.
3. D. Pukazhselvan, V. Kumar and S. K. Singh, *Nano Energy*, 2012, **1**, 566-589.
4. Y.-H. Kim, Y. Zhao, A. Williamson, M. J. Heben and S. B. Zhang, *Phys. Rev. Lett.*, 2006, **96**, 016102.

5. S. K. Bhatia and A. L. Myers, *Langmuir*, 2006, **22**, 1688-1700.
6. E. Tsivion, J. R. Long and M. Head-Gordon, *J. Am. Chem. Soc.*, 2014, **136**, 17827-17835.
7. G. Li, H. Kobayashi, J. M. Taylor, R. Ikeda, Y. Kubota, K. Kato, M. Takata, T. Yamamoto, S. Toh, S. Matsumura and H. Kitagawa, *Nat. Mater.*, 2014, **advance online publication**.
8. W. Zhao, L. Wang, J. Bai, J. S. Francisco and X. C. Zeng, *J. Am. Chem. Soc.*, 2014.
9. S. Meng, E. Kaxiras and Z. Zhang, *Nano Lett.*, 2007, **7**, 663-667.
10. M. Wu, Y. Gao, Z. Zhang and X. C. Zeng, *Nanoscale*, 2012, **4**, 915-920.
11. Q. Sun, Q. Wang, P. Jena and Y. Kawazoe, *J. Am. Chem. Soc.*, 2005, **127**, 14582-14583.
12. Y. Zhao, M. T. Lusk, A. C. Dillon, M. J. Heben and S. B. Zhang, *Nano Lett.*, 2008, **8**, 157-161.
13. G. J. Kubas, *Journal of Organometallic Chemistry*, 2001, **635**, 37-68.
14. J. Niu, B. K. Rao, P. Jena and M. Manninen, *Phys.Rev.B*, 1995, **51**, 4475-4484.
15. J. Niu, B. K. Rao and P. Jena, *Phys. Rev. Lett.*, 1992, **68**, 2277-2280.
16. Q. Sun, P. Jena, Q. Wang and M. Marquez, *J. Am. Chem. Soc.*, 2006, **128**, 9741-9745.
17. A. Du, Z. Zhu and S. C. Smith, *J. Am. Chem. Soc.*, 2010, **132**, 2876-2877.
18. W.-Q. Deng, X. Xu and W. A. Goddard, *Phys. Rev. Lett.*, 2004, **92**, 166103.
19. M. Wu, Q. Wang, Q. Sun and P. Jena, *J. Phys. Chem. C*, 2013, **117**, 6055-6059.
20. X. Wu, Y. Gao and X. C. Zeng, *J. Phys. Chem. C*, 2008, **112**, 8458-8463.
21. Y. Gao, X. Wu and X. C. Zeng, *Journal of Materials Chemistry A*, 2014, **2**, 5910-5914.
22. Z. Tu, M. Wu and X. C. Zeng, *J Phys Chem Lett*, 2017, **8**, 1973-1978.
23. NIST Chemistry WebBook, [webbook.nist.gov](http://webbook.nist.gov)  
[https://en.wikipedia.org/wiki/Heat\\_of\\_combustion](https://en.wikipedia.org/wiki/Heat_of_combustion)    <https://en.wikipedia.org/wiki/Hythane>
24. R. B. Getman, Y.-S. Bae, C. E. Wilmer and R. Q. Snurr, *Chemical Reviews*, 2012, **112**, 703-723.
25. T. A. Makal, J.-R. Li, W. Lu and H.-C. Zhou, *Chemical Society Reviews*, 2012, **41**, 7761-7779.
26. Y. Peng, V. Krungleviciute, I. Eryazici, J. T. Hupp, O. K. Farha and T. Yildirim, *J. Am. Chem. Soc.*, 2013, **135**, 11887-11894.
27. Y. He, W. Zhou, G. Qian and B. Chen, *Chemical Society Reviews*, 2014, **43**, 5657-5678.
28. H. Wu, W. Zhou and T. Yildirim, *J. Am. Chem. Soc.*, 2009, **131**, 4995-5000.
29. F. Gándara, H. Furukawa, S. Lee and O. M. Yaghi, *J. Am. Chem. Soc.*, 2014.
30. J. A. Mason, J. Oktawiec, M. K. Taylor, M. R. Hudson, J. Rodriguez, J. E. Bachman, M. I. Gonzalez, A. Cervellino, A. Guagliardi, C. M. Brown, P. L. Llewellyn, N. Masciocchi and J. R. Long, *Nature*, 2015, **527**, 357-361.
31. M. Savage, I. da Silva, M. Johnson, J. H. Carter, R. Newby, M. Suyetin, E. Besley, P. Manuel, S. Rudić, A. N. Fitch, C. Murray, W. I. F. David, S. Yang and M. Schröder, *J. Am. Chem. Soc.*, 2016.
32. W. Menghao, W. Zhijun, L. Junwei, L. Wenbin, F. Huahua, S. Lei, L. Xin, P. Minghu, W. Hongming, D. Mircea, F. Liang and L. Ju, *2D Materials*, 2017, **4**, 015015.
33. G. Kresse and J. Furthmüller, *Phys.Rev.B*, 1996, **54**, 11169-11186.
34. G. Kresse and J. Furthmüller, *Comp. Mater. Sci.*, 1996, **6**, 15-50.
35. P. E. Blöchl, *Phys.Rev.B*, 1994, **50**, 17953-17979.
36. J. P. Perdew, K. Burke and M. Ernzerhof, *Phys. Rev. Lett.*, 1996, **77**, 3865-3868.
37. S. Grimme, *J. Comp. Chem.*, 2006, **27**, 1787-1799.
38. M. Wu, H. Fu, L. Zhou, K. Yao and X. C. Zeng, *Nano Lett.*, 2015, **15**, 3557-3562.
39. Q. Wang and P. Jena, *J. Phys. Chem. Lett.*, 2012, **3**, 1084-1088.
40. W. Liu, Y. H. Zhao, J. Nguyen, Y. Li, Q. Jiang and E. J. Lavernia, *Carbon*, 2009, **47**, 3452-3460.
41. J. Cai, P. Ruffieux, R. Jaafar, M. Bieri, T. Braun, S. Blankenburg, M. Muoth, A. P. Seitsonen, M.

- Saleh, X. Feng, K. Müllen and R. Fasel, *Nature*, 2010, **466**, 470.
42. M. Wu, X. C. Zeng and P. Jena, *J. Phys. Chem. Lett.*, 2013, **4**, 2482-2488.
43. M. Wu, Y. Pei, J. Dai, H. Li and X. C. Zeng, *J. Phys. Chem. C*, 2012, **116**, 11378-11385.
44. M. Wu, Y. Pei and X. C. Zeng, *J. Am. Chem. Soc.*, 2010, **132**, 5554-5555.
45. M. Wu, A. K. Kandalam, G. L. Gutsev and P. Jena, *Phys.Rev.B*, 2012, **86**, 174410.

## Table of Contents



Mixing hydrogen and methane gas may significantly increase or even double the energy storage capacity